

PACS numbers: 52.50.Jm; 52.38.Dx; 52.38.Ph
DOI: 10.1070/QE2011v041n10ABEH014649

Simulation of experimental investigations of X-ray spectral path lengths on Iskra-5 laser facility

S.A. Bel'kov, O.O. Sharov

Abstract. **We describe an improved Slater average-ion model employed in the numerical-theoretical analysis of experimental data, which were obtained in the investigation of X-ray spectral path lengths performed on the Iskra-5 laser facility at the All-Russian Scientific Research Institute of Experimental Physics (VNIIEF). The proposed model permits determining the spectral characteristics of the X-ray radiation with an accuracy of a few electronvolts. We outline the results of simulations of experiments with X-ray radiation-heated aluminium and germanium specimens of initial thickness of ~0.1 mm, in which absorption lines arising from 1s–2p transitions in Al and the absorption band arising from 2p–3d transitions in Ge were recorded.**

Keywords: *laser-produced plasma, X-ray absorption spectroscopy, X-ray radiation path lengths, Slater average-ion model.*

1. Introduction

Determination of X-ray radiation transfer in a hot substance is one of the problems of plasma physics that is much investigated both theoretically and experimentally. Of special significance for the understanding of how targets should be used in laser fusion and other high energy density physics researches is the 50–100 eV temperature range. To theoretically simulate the X-ray radiation transfer at these temperatures requires knowing in detail the structure of atoms and the shape of spectral lines as well including many-particle interactions in plasma. The complexity of these calculations generates a need for the experimental verification of several simplifying assumptions employed in existing numerical-theoretical models. Not only are the experimental investigations of X-ray transfer in a heated substance of significance in its own right, but they also make it possible to develop the simulation models, thereby providing the means of estimating the transfer in a broader parameter range not covered by experiments. In recent years, experimental studies of radiation transfer in a heated substance with the use of high-power laser facilities are actively performed in many laboratories around the world [1–5]. At the VNIIEF this research is carried out on the Iskra-5 laser facility [6].

S.A. Bel'kov, O.O. Sharov Russian Federal Nuclear Centre 'All-Russian Research Institute of Experimental Physics' (VNIIEF), prosp. Mira 37, 607188 Sarov, Nizhnii Novgorod region, Russia; e-mail: belkov@otd13.vniief.ru, rvtt@runbox.com

Received 3 May 2011; revision received 11 August 2011
Kvantovaya Elektronika **41** (10) 901–905 (2011)
Translated by E.N. Ragozin

Important features of laser-produce plasmas obtained in experiments are a short lifetime and an insignificant optical thickness, with the effect that the local thermodynamic equilibrium approximation is inapplicable to the description of its emissive properties. The latter circumstance lent impetus to the development of kinetic approaches in the description of ionisation in plasmas. The solution of kinetic equations in the framework of a chemical bond model, which considers the evolution of the distribution of ions with different sets of electron shell occupation numbers, runs into serious computational difficulties arising from the high dimensionality of the system of equations. To overcome these difficulties, advantage is taken of the models in which the entire set of ions in excited and ionised states is replaced by a single 'average' ion, whose shell populations are equal to the average shell populations of the entire distribution.

Among different models for calculating the atomic characteristics of an average ion, it is expedient to single out the class of Slater models. Slater ion models reproduce reasonably well the main spectral features of the radiation of multiply charged ion plasma. They are sufficiently universal and permit calculating the spectral plasma characteristics both under local thermodynamic equilibrium and in its absence. Furthermore, these models are rather simple, which provides the possibility of using them in the numerical simulation of radiating nonequilibrium transient plasmas in radiative gas dynamics programs.

The present paper is dedicated to the simulation of experiments in X-ray radiation transfer in heated aluminium and germanium performed on the Iskra-5 facility; our simulations rely on the Slater average-ion model employed at the VNIIEF. The numerical-theoretical analysis of experiments was carried out with the aid of a one-dimensional gas dynamic program, SNDP, which takes into account the absorption of laser radiation, plasma motion in a two-temperature approximation, electron and ion thermal conduction with electron and ion temperature relaxation, the spectral transfer of nonequilibrium radiation under diffusion approximation, and ionisation kinetics in the average-ion approximation [7, 8].

2. Average-ion model

The energy of an isolated ion is made up of three parts: the kinetic energy of bound electrons T, an electron–nucleus interaction energy V_n, and an electron–electron interaction energy V_{ee}. For the energy of an ion with an electron configuration

$$\{C\} = \prod_k q_k^{P_k} = \{q_1^{P_1}, q_2^{P_2}, ..., q_k^{P_k}, ...\},$$

where q_k is the set of quantum numbers of kth electron shell and P_k is its population, the Slater model gives the following expression (in atomic units) [9]:

$$E = T + V_n + V_{ee} = \sum_k P_k \frac{Z_k^2}{2n_k^2} - \sum_k P_k \frac{Z_k}{2n_k^2} Z + V_{ee}. \quad (1)$$

Here, Z_k is the effective nuclear charge for kth shell electrons; n_k is the principal shell number; and Z is the nuclear charge of the ion.

The electron–electron interaction energy V_{ee} is the sum of Hartree energy V_H and the energy of exchange-correlation interaction V_{xc}:

$$V_{ee} = V_H + V_{xc} = \frac{1}{2}\sum_{k,k'} P_k P_{k'} \{k,k'\} - \frac{1}{2}\sum_k P_k^2 \{k,k\}$$

$$= \frac{1}{2}\sum_{k,k'} P_k (P_{k'} - \delta_{kk'})\{k,k'\}, \quad (2)$$

where $\delta_{kk'}$ is the Kronecker symbol and $\{k, k'\}$ is the linear combination of Slater integrals [10].

Effective nuclear charges are found from the minimum total-ion-energy condition and are calculated by the formula

$$Z_k = Z - \sum_{k'} \sigma_{kk'} (P_{k'} - \delta_{kk'}), \quad (3)$$

where $\sigma_{kk'}$ is the universal matrix of screening constants.

The binding energy ε_k of an electron is calculated as the difference of ion energies with and without this electron:

$$\varepsilon_k = E\{C\} - E\{C'\}, \quad (4)$$

where

$$C' = \prod_{k'} q_{k'}^{P_{k'} - \delta_{kk'}}.$$

It may be shown that the electron binding energy is approximated, correct to the second variation of shell population, by the derivative of the total ion energy with respect to the corresponding population,

$$\varepsilon_k = \frac{\partial E}{\partial P_k}\Big|_{1/2}, \quad (5)$$

where the derivative $\partial E/\partial P_k$ is calculated at the point $C' = \prod_k q_{k'}^{P_{k'} - \delta_{kk'}/2}$ (derivative 'at 1/2'). The accuracy of approximation is equal to $\sigma_{kk}^2/(8n_k^2)\delta P^2$ and amounts to a fraction of an electronvolt. Similarly, the difference

$$\varepsilon_{ij} = \frac{\partial E}{\partial P_j}\Big|_{1/2} - \frac{\partial E}{\partial P_i}\Big|_{1/2} \quad (6)$$

corresponds to the energy of a one-electron transition to within a fraction of an electronvolt. The latter expression significantly simplifies calculations, because it permits using the binding energies (5) without recalculating the ion energy in the final state of every transition.

The Kronecker symbol in formula (3) for the effective charge is the same as in expression (2) for the electron–electron interaction energy V_{ee}: it is responsible for the correction for the excess Coulomb contribution to the self-consistent field from the electron under consideration and is introduced to take into account the exchange-correlation hole [11]. According to our calculations, the use of formula (3) shifts absorption lines to the hard domain in comparison with experiment. To avoid this, in formula (3) we introduced a coefficient $\alpha(Z)$ dependent on the element's atomic number, which was selected in such a way as to provide the best fit of calculated absorption line peaks to the experimental ones:

$$Z_k = Z - \sum_{k'} \sigma_{kk'} (P_{k'} - \alpha(Z)\delta_{kk'}). \quad (7)$$

For a basic set of screening constants we took the matrix σ^F proposed by Faussurier et al. [9, 12], which takes into account the splitting of electron energy levels in orbital quantum number l. The number of electron shells and hence the number of equations of ionisation kinetics increases with a rise in the maximum principal quantum number n_{max} as $n_{max}(n_{max}+1)/2$. At the same time, the l-splitting of the outer shell levels ($n > 6$) amounts to no more than several percent of the spacing between levels even for elements like lead. This signifies that advantage can be taken of a model without splitting in orbital quantum number when outer shells are involved. The matrix σ^M of l-degenerate screening constants for levels with principal quantum numbers up to 10 inclusive was presented by More [13]. By supplementing the inner part of the σ^F matrix with the values of σ^M, we obtain the $\sigma_{kk'}$ matrix, where the symbols k and k' now denote either a combination of quantum numbers nl or only the principal quantum number.

The matrix σ^F of screening constants was obtained by fitting the ion energy structure calculated by the Slater model to the structure calculated by the nonrelativistic Hartree–Fock model. For heavy elements, account must be taken of relativistic effects, which were introduced as corrections to binding energies $\varepsilon_k \to \varepsilon_k + \delta\varepsilon_k^{rel}$ calculated with the aid of the screening matrix:

$$\delta\varepsilon_k^{rel} = \varepsilon_k^{rel} - \frac{1}{\alpha^2} + \frac{Z_k^2}{2n_k^2}, \quad (8)$$

where α is the fine structure constant;

$$\varepsilon_k^{rel} = \frac{1}{\alpha^2}\left\{1 + \frac{(Z_k\alpha)^2}{\left[\sqrt{\kappa_k^2 - (Z_k\alpha)^2} + n_{rk}\right]^2}\right\}^{-1/2}; \quad (9)$$

is the relativistic electron energy level in the Coulomb field of a nucleus of charge Z_k [14]; $|\kappa_k| = j_k + 1/2$; j_k is the total electron momentum; and $n_{rk} = n_k - |\kappa_k|$.

The relativistic corrections may be included in the solution of the equations of ionisation kinetics, but their magnitude is much smaller than the spacing between levels with different l, and the number of equations rises to n_{max}^2 in this calculation. This was the reason why these corrections were determined only in the detailed calculation of specimen's X-ray transmission spectra upon solving the differential kinetic equations.

Interactions with ambient plasma ions affect the energies of bound states and result in the splitting of electron shells and the transition of a part of the bound states to the continuum. The splitting was modelled by introducing a dependence of the shell's statistical weight on the plasma density:

$$D_k = \frac{D_k^0}{1 + a(R_k/R_0)^b}, \quad (10)$$

where D_k^0 is the statistical weight of the shell of an isolated ion; $R_k = n_k^{3/2}\sqrt{l_k + 1/2}/Z_k$ is the radius of kth electron shell; R_0 is the ion-sphere radius; and a, b are constants obtained from the condition of the best fit to models which *ab initio* include the effect of environment. The values of constants a and b for different elements and the technique for their calculations are given in Ref. [15]. The lowering of ionisation potential is determined by the correlation energy E^{ci} of Coulomb ion interaction:

$$\delta\varepsilon^{\text{ci}} = -\frac{\partial E^{\text{ci}}}{\partial\langle Z\rangle}, \tag{11}$$

where $\langle Z\rangle$ is the average ion charge. The method for calculating the ion interaction energy is also described in Ref. [15].

In the general case, solving the kinetic equations of average-ion ionisation yields fractional values of the average populations of electron shells. X-ray absorption coefficients may be calculated directly from the average shell populations, but in this case account must be taken of the statistical broadening of energy levels defined by the thermodynamic fluctuations of shell occupation numbers. By the order of magnitude the statistical broadening corresponds to the derivative of electron binding energy with respect to level population and amounts to several percent of the binding energy under the typical conditions of experiments involving laser-produces plasmas (for a temperature of 0.1 keV and a density of 0.1 g cm^{-3}). For ~1-keV energies it amounts to tens of electronvolts, and the resultant absorption lines turn out to be the envelopes of lines corresponding to individual electron configurations. This calculation does not permit identifying the absorption peaks corresponding to ions of different charge, and so we recovered the distribution of ions with integer shell populations. In this case, electrons were considered to be independent, and the probability of realisation of a specific configuration was calculated as the product of one-electron probabilities. Furthermore, the probability that m electrons resided in the kth shell was assumed to obey the binomial law [16]

$$f_k^m = \binom{D_k}{m} p_k^m (1 - p_k)^{D_k - m}, \tag{12}$$

where D_k is the statistical weight of the shell and $p_k = P_k/D_k$ is the degree of shell filling.

In the calculation of the spectral absorption coefficient, we included: photoabsorption using the Kramers formula with Gaunt correction factor borrowed from Ref. [17], line absorption [18], inverse bremsstrahlung using the Kramers formula with temperature-averaged Gaunt correction factor in the Born–Elvert approximation [19], and the Compton scattering [14].

3. Simulation of experiments

The X-ray transfer in a heated substance was experimentally investigated using the technique of point absorption spectroscopy on the Iskra-5 facility. In the first experiments on this facility, specimens were heated by the radiation of one of its channels. We shall consider the single-channel experiment in which use was made of an aluminium specimen with an initial thickness of 0.15 μm. A diagrammatic view of the target assembly, experiment details, as well as its results are outlined in Ref. [6]. In the analysis of the experiment, calculations were made of the X-ray radiation flux emanating from the converter, with the subsequent determination of the dynamics of specimen heating by the resultant X-ray radiation. A Planck spectrum with temperature defined by the intensity of X-ray converter radiation was prescribed as a boundary condition for the incident radiation on the specimen's surface.

In experiment the specimen expands and does not manage to get heated: at the moment the X-ray pulse reaches its peak, the difference of temperatures at different points over the specimen's depth is two-fold and the density difference is six-fold. The highest plasma temperature is 25 eV, the average density is close to 0.1 g cm^{-3}. The calculated transmittance is in satisfactory agreement with the experimentally recorded one (Fig. 1).

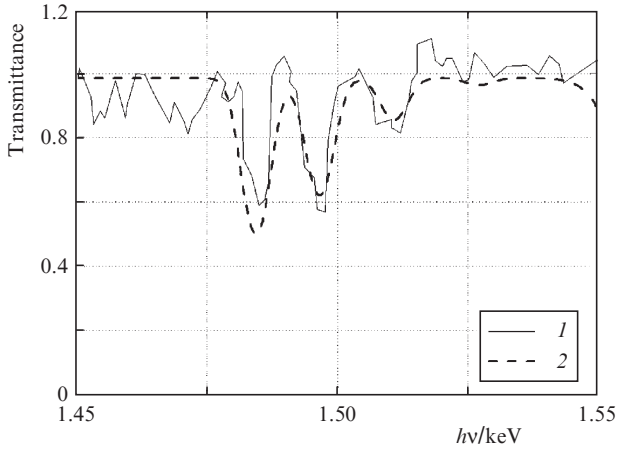

Figure 1. Transmission spectrum of the plasma of a 0.15-μm-thick aluminium specimen in a one-channel experiment (*1*) and in simulations (*2*).

In single-channel experiments, the amount of soft X-ray radiation acting on the specimen under investigation is insufficient to heat it up to a high temperature. That is why an experiment was designed, which involved the use of four channels of the Iskra-5 facility for the formation of a heating X-ray pulse. In the first multichannel experiments, the specimen's heating was one-sided. Subsequently, targets for two-sided heating were made. The geometry of the target assembly was described in Ref. [6]. It was invariable in all experiments, only the thickness of the specimen under study, the shape of laser pulses, and the probe delay were varied.

According to our simulations, the specimens subjected to one-sided heating in four-channel experiments are heated much more uniformly than in single-channel experiments. The nonuniformities of temperature and density distributions are equal to about 10%. Figure 2 shows the transmittance of an aluminium specimen with an initial thickness of 0.1 μm in one of these experiments at the instant the X-ray pulse reaches its peak. In this experiment the energy of laser radiation introduced into the converter box was equal to 700 J, the pulse duration was 0.5 ns, and the delay of the X-ray pulse was 0.75 ns. At the peak of the laser pulse the average calculated temperature of the specimen was equal to 45 eV and the density was 0.023 g cm^{-3}.

In experiments with two-sided specimen heating, radiation path lengths were investigated in 0.09- and 0.11-μm-thick aluminium specimens and in a 0.14-μm-thick germanium specimen. The total energy of laser radiation in experiments

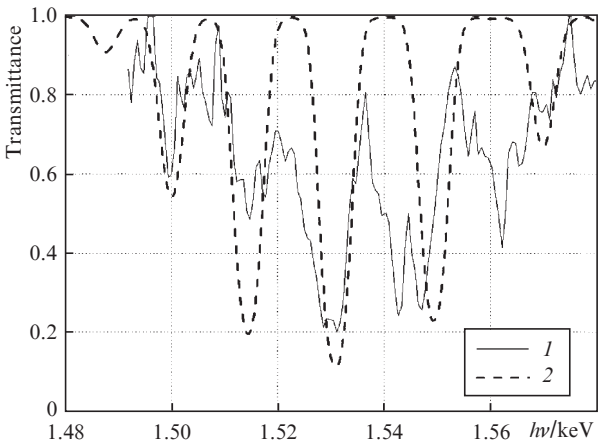

Figure 2. Transmission spectrum of the plasma of a 0.1-μm-thick aluminium specimen in an experiment with one-sided heating (*1*) and in simulations (*2*).

with aluminium specimens was equal to 700 and 900 J, respectively, and to 900 J in experiments with germanium specimens. The pulse duration in the channels was equal to 0.32–0.38 ns and 0.48–0.93 ns for aluminium and to 0.60–0.75 ns for germanium. The X-ray pulse delays were equal to 0.75, 0.7, and 0.6 ns. The spectra recorded in experiments with aluminium are given in Fig. 3. The spectrometer used in the experiment with the 0.11-μm-thick specimen had a higher resolution than that used in the experiment with the 0.09-μm-thick specimen, and the spectrum in Fig. 3b exhibits more features than the spectrum in Fig. 3a. One can see that the calculation models the experimental data with a satisfactory accuracy. The simulation of germanium transmittance [Fig. 4, curve (*2*)] also provides a reasonable description of the positions of the lines arising from the 2p–3d transition (the 1.20–1.25 keV range) and of the absolute magnitude of absorption due to these lines.

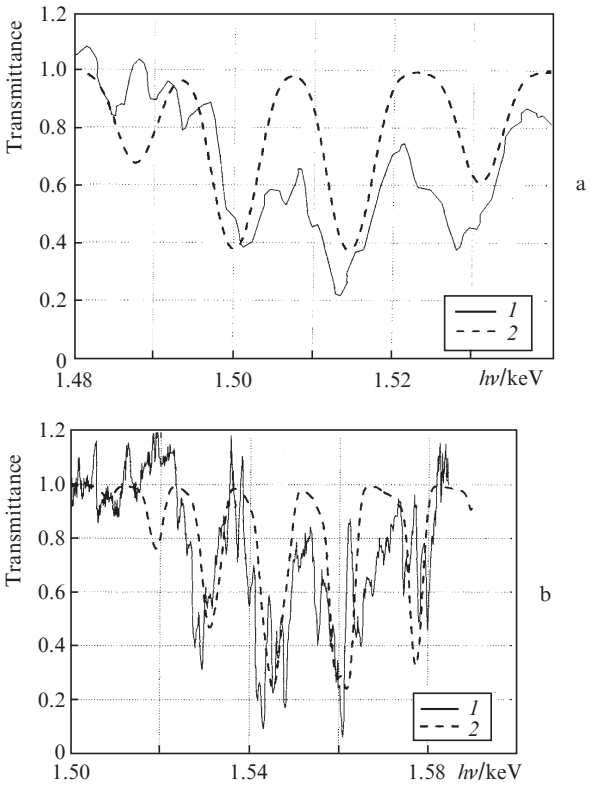

Figure 3. Transmission spectra of the plasmas of 0.09-μm (*a*) and 0.11-μm-thick aluminium specimens in experiments with two-sided heating (*1*) and in simulations (*2*).

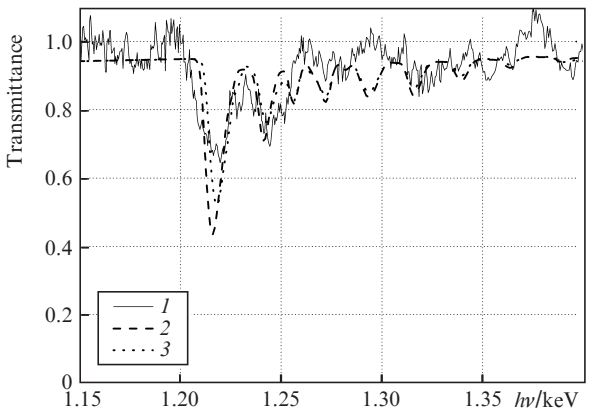

Figure 4. Transmission spectrum of the plasma of a 0.14-μm thick germanium specimen in the experiment with two-sided heating (*1*), in the simulation for the instant of the X-ray pulse peak (*2*), and in the simulation averaged over the X-ray pulse duration (*3*).

In all of the simulation spectra presented, we show the transmittance at the instant of the X-ray pulse peak. However, the duration of the probe pulses in experiments was comparable to the duration of heating X-ray pulses and to the time delay of the probe pulses. In order to reveal the effect of the finiteness of X-ray pulse duration on the results of spectra determination, we performed a calculation to take it into account.

Figure 4 shows the calculated plasma transmittance in the experiment with a germanium specimen; the transmittance was averaged over the X-ray pulse duration, which was equal to 0.72 ns. One can see that the inclusion of the finite pulse width has only a minor effect on the data. The transmittance in the lines became somewhat higher and the calculated dependence became closer to the experimental one, but these changes are insignificant.

4. Conclusions

A new way for including the exchange-correlation interaction of electrons in the average-ion model was proposed in this paper, which makes it possible to determine the spectral characteristics of radiation correct to a few electronvolts. For this purpose, an additional parameter dependent on the atomic element number was introduced into the screening matrix. Realised in the model is a possible method of reconstructing the distribution of ions with integer electron shell populations, which proceeds from the information about average shell populations. This permitted resolving absorption spectral lines corresponding to ions of different charge for internal transitions in Al and Ge. We presented the results of simulations of X-ray transmission spectra in one- and four-channel experiments to investigate the opacity of specimens with thicknesses of the order of 0.1 μm. The proposed model

was shown to adequately describe these experiments. The model elaborated in this work is intended for the description of processes occurring in laser fusion targets.

Acknowledgements. The authors express their appreciation to N. A. Suslov for presenting experimental data.

References

1. Foster J.M., Hoarty D.J., Smith C.C., et al. *Phys. Rev. Lett.*, **67** (23), 3255 (1991).
2. Eidmann K., Schwanda W., Foldes I.B., et al. *J. Quantum Spectr. Radiat. Transfer*, **51** (1/2), 77 (1994).
3. Perry T.S., Budil K.S., Cauble R., et al. *J. Quantum Spectr. Radiat. Transfer*., **54** (1/2), 317 (1995).
4. Chenais-Popovics C., Gilleron F., Fajardo M., et al. *J. Quantum Spectr. Radiat. Transfer.*, **65**, 117 (2000).
5. Jiamin Yang, Yaonan Ding, Jun Yan, et al. *Phys. Plasmas*, **9** (2), 678 (2002).
6. Bondarenko S.V., Garanin R.V., Zhidkov N.V., et al. *Kvantovaya Elektron.* (in print) [*Quantum Electron.* (in print)].
7. Bel'kov S.A., Dolgoleva G.V. *Voprosy Atomnoi Nauki i Tekhniki. Ser. Mat. Model. Fiz. Protsessov*, **1**, 59 (1992).
8. Bel'kov S.A., Gasparyan P.D., Kochubei Yu.K., Mitrofanov E.I. *Zh. Eksp. Teor. Fiz.*, **111** (2), 495 (1997).
9. Faussurier G., Blancard C., Decoster A. *J. Quantum Spectr. Radiat. Transfer.*, **58**, 2, 233 (1997).
10. Sobel'man I.I. *An Introduction to The Theory of Atomic Spectra* (Oxford: Pergamon Press, 1973; Moscow: Fizmatlit, 1963).
11. http://cmt.dur.ac.uk/sjc/thesis_ppr/.
12. Fassurier G., Blancard C., Renaudin P. *High Energy Density Phys*., **4**, 114 (2008).
13. More R.M. *J. Quantum Spectr. Radiat. Transfer.*, **27**, 345 (1982).
14. Berestetskii V.B., Lifshits E.M., Pitaevskii L.P. *Quantum Electrodynamics* (Oxford: Pergamon Press, 1982; Moscow: Nauka, 1989).
15. Bel'kov S.A., Bondarenko S.V., Mitrofanov E.I. *Kvantovaya Elektron*., **30**, 963 (2000) [*Quantum Electron.,* **30**, 963 (2000)].
16. Takabe H., Nishikawa T. *J. Quantum Spectr. Radiat. Transfer.*, **51** (1/2), 379 (1994).
17. Zel'dovich Ya.B., Raizer Yu.P. *Physics of Shock Waves and High-Temperature Hydrodynamic Phenomena* (New York: Academic Press, 1966, 1967; Moscow: Nauka, 1966).
18. Itoh M., Yabe T., Kiyokawa S. *Phys. Rev. A*, **35**, 233 (1987).
19. Nikiforov A.F., Novikov V.G., Uvarov V.B. *Kvantovo-statisticheskie modeli vysokotemperaturnoi plazmy i metody rascheta rosselandovykh probegov i uravnenii sostoyaniya* (Quantum-Statistical Models of High-Temperature Plazma and Methods for Calculating Rosseland Lengths and Equations of State) (Moscow: Fizmatlit, 2000).